

THREE ELEMENT DUAL SEGMENT TRIANGULAR DIELECTRIC RESONATOR ANTENNA FOR X-BAND APPLICATIONS

A. Gupta¹, R. K. Gangwar^{2, *}, and S. P. Singh¹

¹Department of Electronics Engineering, Indian Institute of Technology, Banaras Hindu University, Varanasi 221005, India

²Department of Electronics Engineering, Indian School of Mines, Dhanbad 826004, India

Abstract—A wideband dual segment three element triangular dielectric resonator antenna (TDRA) has been proposed for applications in X-band. Proposed antenna has been fabricated and tested. The simulation study of the antenna is carried out using Ansoft HFSS simulation software. The simulation results for input characteristics and radiation patterns of the proposed antenna are compared with corresponding experimental results at the resonant frequency. The simulation results are in agreement with the measurement results. The return loss-frequency characteristics of the proposed antenna are also compared with those of single element, and three element TDRAs.

1. INTRODUCTION

In 1939, R. D. Richtmyer showed that unmetallized dielectric objects could function similar to metallic cavities, which he called dielectric resonators [1]. The DRA is an open resonating structure, fabricated from a low loss dielectric material. It offers advantages such as small size, high radiation efficiency due to the absence of conductor losses simple geometry, small size, flexible feed arrangement, wide range of material dielectric constant, ease of excitation and easily controlled characteristics As compared with microstrip antenna, the DRA has wider impedance bandwidth and better efficiency due to absence of surface wave [2–5].

Received 29 August 2012, Accepted 31 October 2012, Scheduled 1 November 2012

* Corresponding author: Ravi Kumar Gangwar (ravi.gangwar.ece07@itbhu.ac.in).

Bandwidth enhancement is becoming the major design consideration for most practical applications of dielectric resonator antennas [5]. The techniques used to improve the bandwidth of the DRAs include changing the aspect ratio of DRA, modifying feed geometries, employing multi-segments and stacked DRAs and by varying the dielectric constant of DRA material [6, 7]. The gain, bandwidth and radiation performances of DRA can be modified by using stacked or stair shaped DRA instead of a single DRA. Stacking of DRAs is an efficient technique to improve the gain, bandwidth and radiation performances [8–11]. For wide-band applications, DRAs having lower dielectric constant values are preferred. This results in weak coupling. Multi-segment DRAs can be used to overcome this problem [6].

For monopole type radiation pattern, only a few studies on DRAs are reported in the literature. The dielectric ring resonator is a common DRA structure that radiates monopole like field [12]. Composite cylindrical DRAs have been investigated as broadband variants of low profile monopole type DRAs [13]. Three element multilayer cylindrical dielectric resonator antennas can offer an impedance bandwidth of $\sim 47\%$ with monopole like radiation pattern [14]. Similarly, composite hemispherical DRA which produces monopole type radiation over a large bandwidth has also been investigated [15, 16]. Further, a wideband four element rectangular dielectric resonator antenna array for 5.0 GHz WLAN and WiMAX band with monopole like radiation pattern has been studied through simulation [17].

This paper presents the simulation and experimental studies of a three element dual segment triangular DRA (TDRA), which is fed by a 50Ω coaxial probe and produces a monopole like radiation pattern over wide bandwidth. The simulation study of the proposed antenna array is carried out using commercially available Ansoft HFSS software. Proposed antenna produces a monopole like radiation pattern over wide bandwidth having resonant frequency of 10.8 GHz. The simulation results are compared with measured results at the resonant frequency of 10.8 GHz. The variation of simulated values of return loss versus frequency of the proposed antenna are also compared with those of single element, and three element TDRA.

2. THE ANTENNA GEOMETRY

The advantage of the triangular DRA is that for a given height and resonant frequency, it offers a smaller area than either a cylindrical or rectangular DRA [18, 19]. Thus, it is advantageous for an antenna array design since a larger range of spacing between elements is allowed.

The resonant frequency of the TM_{mnl} mode in an equilateral-triangular DR on a ground plane is approximately given by [18, 20, 21].

$$f_{lmn} = \frac{1}{2\sqrt{\epsilon\mu}} \left[\left(\frac{4}{3a} \right)^2 (m^2 + mn + n^2) + \left(\frac{\rho}{2h} \right)^2 \right]^{\frac{1}{2}} \quad (1)$$

This can also be written as

$$f_{mn} = \frac{c}{2\sqrt{\epsilon_r}} \left[\left(\frac{4}{3a} \right)^2 (m^2 + mn + n^2) + \left(\frac{\rho}{2h} \right)^2 \right]^{\frac{1}{2}} \quad (2)$$

where c is the speed of light, ϵ_r the dielectric constant, a the length of each side of the triangle, and h the height of the resonator. The resonant frequency indices m and n are used here instead of m , and n and l because the third index l is dependent on the values of m and n . The indices l , m , and n satisfy the condition $l + m + n = 0$, but they all cannot be zero simultaneously. $\rho = 1$ for the fundamental TM_{10-1} mode.

Four configurations of equilateral triangular DRA/DRAs are taken for simulation study using FEM based Ansoft HFSS software. First is the single element equilateral triangular DRA (TDRA) shown in Fig. 1 with $a = 12.6$ mm and $h = 6$ mm which operates at the central frequency of 7.185 GHz. The DRA is designed using Alumina (Al_2O_3) that has dielectric constant ϵ_r of 9.8 with ground plane of dimensions 50 mm \times 50 mm. The single element TDRA is assumed excited by a 50 Ω coaxial probe, which touches the corner edge of the antenna. The second is the three-element TDRA shown in Fig. 2. Each element of the three element TDRA is of same size as the first configuration and assumed constructed of the same material. The elements of the three element TDRA are assumed centrally excited by a 50 Ω coaxial probe which touches the corner edges of all the three elements. The third is the dual segment TDRA shown in Fig. 3 with $a = 12.6$ mm and total height $H (= h_1 + h_2) = 6.0$ mm. Dual segment TDRA consists of two segments. The first segment of height $h_1 = 1.5$ mm is designed using Teflon sheet of dielectric constant ϵ_r of 2.08. The second segment of height $h_2 = 4.5$ mm consists of Alumina (Al_2O_3) that has dielectric constant ϵ_r of 9.8. Teflon segment having low dielectric constant is inserted between the ground plane and the second segment made of Alumina to enhance the bandwidth [6]. The single element dual segment TDRA is assumed excited by a 50 Ω coaxial probe, which touches the corner edge of the antenna. The fourth is the proposed three element dual segment TDRA shown in Fig. 4 with $a = 12.6$ mm and total height $H (= h_1 + h_2) = 6.0$ mm. Each element of the three element dual segment TDRA is of same size as the third

configuration and assumed constructed of the same materials. The elements of the proposed structure are packed together in a compact way on a metallic ground plane of dimensions $14\text{ cm} \times 12\text{ cm}$ and are centrally excited by a $50\ \Omega$ coaxial probe which touches the corner edges of all the three elements of the proposed structure. The height of the probe above the ground plane for different antenna structures is determined through extensive simulation to obtain minimum return loss at the corresponding resonant frequency. The desired height of the probe is found to be 6 mm each for single element and three element TDRAs, whereas it is equal to 4.5 mm and 5 mm respectively for dual segment single element and dual segment three element TDRAs. Fig. 5 shows the photograph of the fabricated structure of the proposed dual segment three element TDRA. The resonant frequency of the TDRA in free space for TM_{10-1} mode computed using Equation (2) is found to be 7.185 GHz .

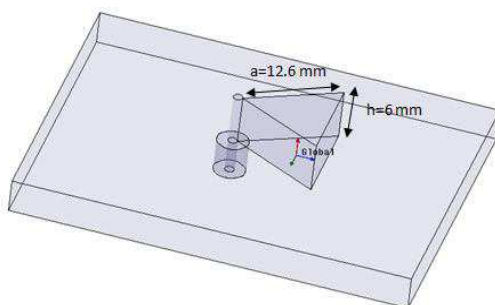


Figure 1. Equilateral TDRA.

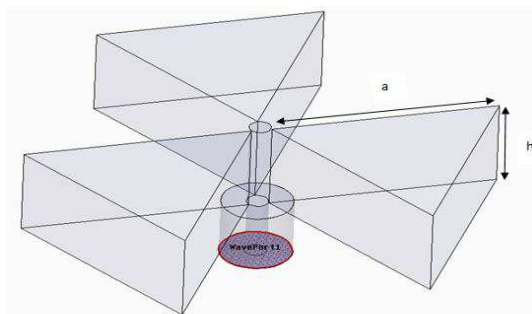


Figure 2. Three element TDRA.

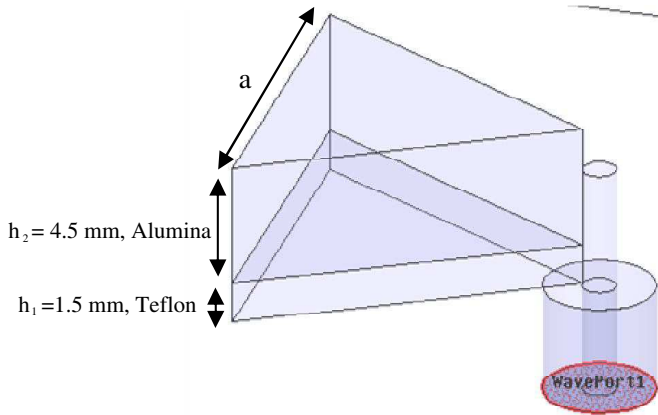


Figure 3. Single element dual segmented TDRA.

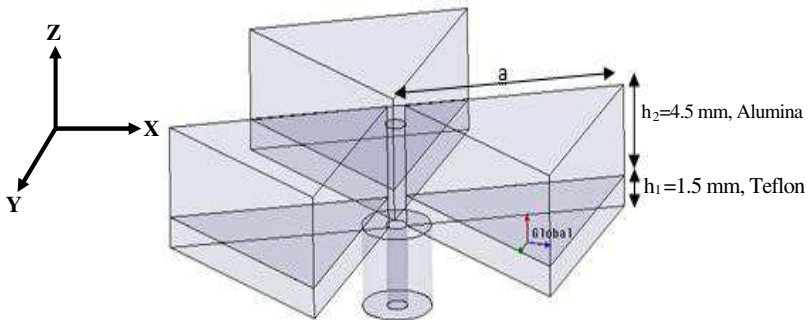


Figure 4. Three element dual segmented TDRA.

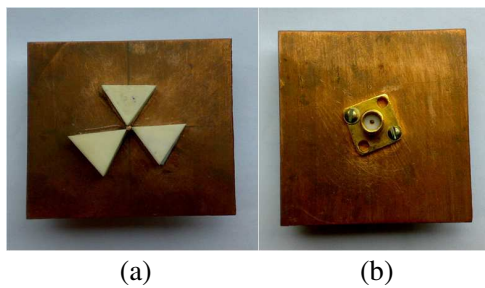


Figure 5. Fabricated structure. (a) Front view. (b) Back view.

3. RESULTS AND DISCUSSION

3.1. Return Loss and Input Impedance Curves

The simulation study of return loss and/or input impedance versus frequency characteristics of the single element, three element, dual segment single element, and proposed dual segment three element TDRA have been carried out using Ansoft HFSS software. Proposed three element dual segment TDRA has been fabricated and tested. Measurement of return loss and input impedance of proposed antenna was carried out over 9–12 GHz range using Agilent PNA series Vector Network Analyzer (Model No. E8364 B).

The simulation results for the return loss of single element, three element, dual segment three element and proposed TDRA are shown in Fig. 6. From Fig. 6 the resonant frequency, operating frequency range and -10 dB return loss bandwidth of the TDRA are extracted and the results are given in Table 1. The simulated values of return loss versus frequency of the proposed three element dual segment TDRA are compared with corresponding measured results as illustrated in Fig. 7.

From Fig. 6 and Table 1, it can be seen that the proposed antenna has the widest bandwidth ($= 22.92\%$) among all. It is also clear that the proposed TDRA has the resonant frequency of 10.8 GHz. From Fig. 6 and Table 1 it can be observed that the single element TDRA

Table 1. Comparison of simulated return loss parameters.

Parameters	Resonant Frequency	Operating frequency range	-10 dB return loss bandwidth
single element TDRA	7.665 GHz	7.275–8.115 GHz	10.92%
three element TDRA	7.713 GHz	7.13–8.3 GHz	14.01%
single element dual segment TDRA	9.06 GHz	8.52–9.96 GHz	15.89%
three element dual segment TDRA	10.8 GHz	9.27–11.67 GHz	22.92%

Table 2. Simulated and measured antenna parameters.

Parameters	Resonant Frequency	-10 dB return loss bandwidth
Simulated	10.8 GHz	22.92%
Measured	10.77 GHz	15.78%

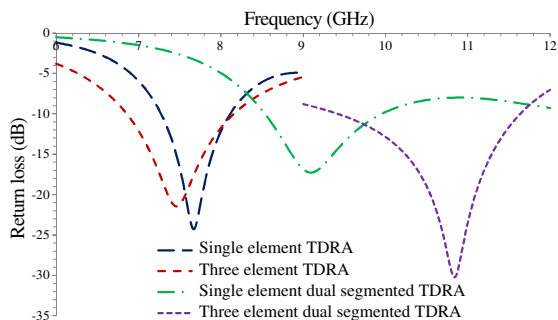


Figure 6. Comparison of values of return loss versus frequency for the TDRAs.

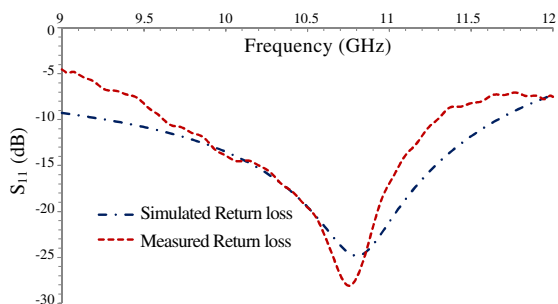


Figure 7. Comparison of measured and simulated return loss characteristics.

covers the frequency range from 7.275 GHz to 8.115 GHz with -10 dB return loss bandwidth of 10.92%, and has the simulated value of resonant frequency of 7.665 GHz which is nearly in agreement with the computed value of 7.185 GHz using Equation (2). Also large frequency shift is observed when comparing the single dual-segment TDRA to the three element dual-segment TDRA. This is because of the generation of very close multiple resonant modes in three element dual-segment TDRA [13–16].

The measured values of return loss of the proposed dual segment TDRA at different frequencies in X-band are in agreement with the simulated results as illustrated in Fig. 7 and Table 2. The simulated return loss value is -24.834 dB at the resonant frequency of 10.8 GHz whereas measured value is -27.985 dB at the resonant frequency of 10.77 GHz.

It has also been found from the study that the simulated value of input resistance at the resonant frequency of proposed TDRA is 48.18Ω , and measured value at the corresponding resonant frequency is 47.39Ω both of which are close to 50Ω impedance of the feeder.

3.2. Near Field Distribution

The simulation study of near field distribution in the proposed three element dual segment TDRA has been carried out at 10.8 GHz using Ansoft HFSS software. When three elements are simultaneously excited using $50\ \Omega$ coaxial probe as shown in Fig. 4, the composite electric and magnetic field distributions in 3D plane look like those shown in Figs. 8(a) and (b) respectively. It is apparent from Fig. 8 that the coaxial probe excites TM_{10-1} dominant mode fields in the antenna elements. Also it can be observed that electric field component face their counter vectors and thus cause no radiation along broadside direction.

The resultant electric field is polarized along z -direction and thus it leads to a vertically polarized radiation surrounding the radiating structure like a quarter wave electric monopole. Since the elements of the antenna composite TDRA structure effectively produces identical radiation fields at 10.8 GHz, uniform monopole-type pattern can be achieved over the full matching bandwidth.

3.3. Far Field Distribution

The radiation patterns (both co-polar and cross-polar) of the fabricated three element dual segment TDRA for $\Phi = 0^\circ$ (x - z plane or H -plane) and $\Phi = 90^\circ$ (y - z plane or E -plane) were measured in anechoic chamber at resonant frequency of 10.8 GHz and simulated using Ansoft HFSS software. The experimental setup is not shown here for brevity. A practical antenna is never 100% polarized in a single mode (linear, circular, etc.). Hence, two radiation patterns of proposed DRA are presented, the co-polar (or desired polarization component) radiation pattern and the cross-polarized radiation pattern for both H - and E -planes. The cross polarized level may be specified for an antenna as the

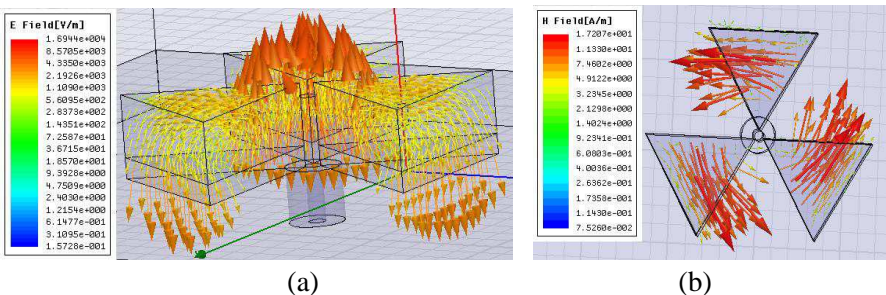


Figure 8. Simulated near field distribution of proposed antenna at 10.8 GHz. (a) E -field. (b) H -field.

power level in negative dB value, indicating how many decibels down this power level is with respect to the desired polarization’s power level. The simulated and measured radiation patterns of the three element dual segment TDRA in *H*- and *E*-planes are shown in Figs. 9 and 10 respectively.

From Figs. 9 and 10 it is clear that trend of variation in the simulated angular patterns of the proposed antenna is similar to that obtained in corresponding experimental patterns, though dynamic range of power level variation in experimental patterns is less than the corresponding range of level variation in the simulated patterns. It can also be observed from Figs. 9 and 10 that no radiation is obtained

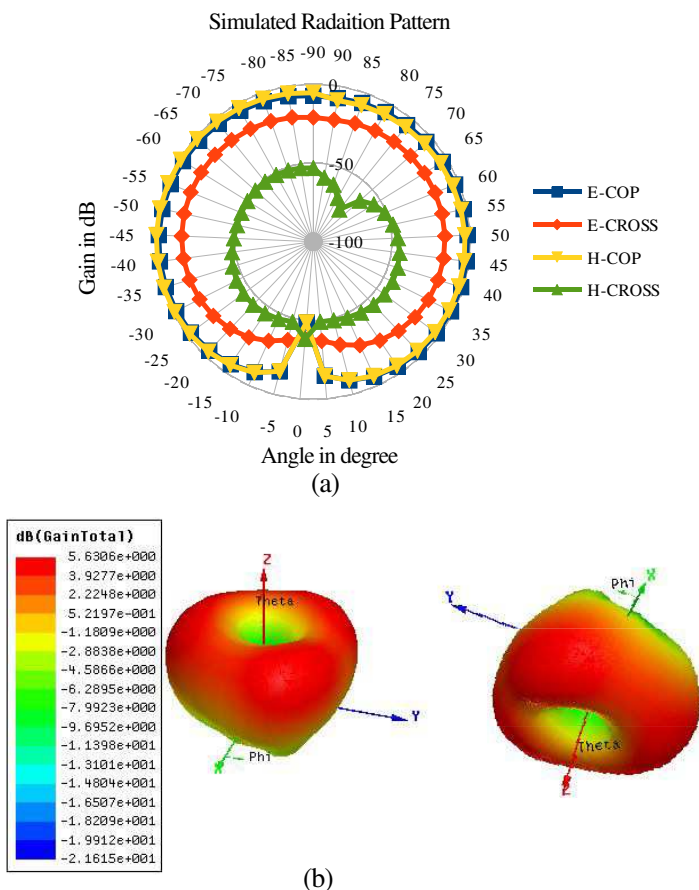


Figure 9. Simulated radiation patterns at 10.8 GHz. (a) Polar plot. (b) 3D plot.

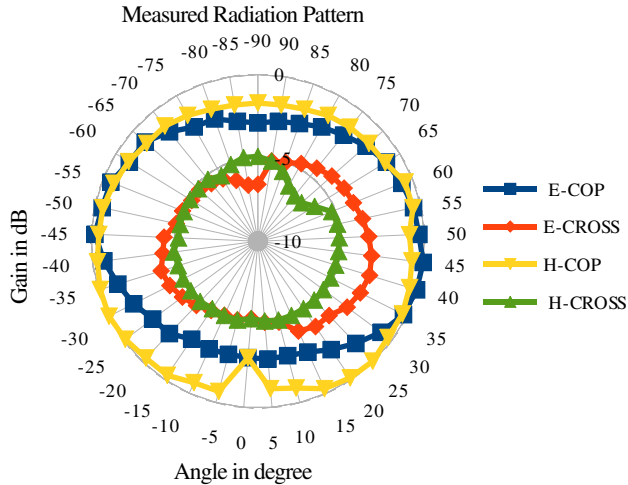


Figure 10. Measured radiation patterns at 10.8 GHz.

along the broadside direction of the antenna because of counteracting E -field distribution in x - y plane within the elements of the antenna. The radiation pattern of the antenna in x - y plane is omni-directional as shown in Fig. 9(b). The deviation in experimental and simulation results may be attributed to fabrication errors like cutting of hard ceramic material (Alumina), use of adhesive material to join antennas, possibility of air gaps between ground plane and Teflon material and between Teflon material and Alumina, probability of improper contact between DRA elements and the coaxial probe, and error in angular orientation of the elements of antenna on the conducting ground plane in the experiment, and error in manual measurement of radiation patterns.

4. CONCLUSION

In this paper, a wideband dual segment three element TDRA has been studied experimentally as well as through simulation using Ansoft HFSS software. Further, the simulated return loss-frequency characteristics of the proposed antenna have been compared with those of single element, three element, and single element dual segment TDRA. From the study it is inferred that the bandwidth of the proposed antenna has been found to be the widest among all configurations (= 22.92% through simulation, though experimental bandwidth is less) and it provides wide angle coverage considering 10 dB angular width at the cost of no broadside radiation. The results

obtained may be useful for designing and developing antennas for WLAN systems, subsurface communication, geophysical exploration, biomedical telemetry, and for mobile terrestrial and aerospace communication systems.

REFERENCES

1. Richtmyer, R. D., "Dielectric resonators," *J. Appl. Phys.*, Vol. 10, 391–398, June 1939.
2. Long, S. A., M. W. McAllister, and L. C. Shen, "The resonant cylindrical dielectric cavity antenna," *IEEE Transactions on Antennas and Propagation*, Vol. 31, 406–412, May 1983.
3. Petosa, A., A. Ittipiboon, Y. M. M. Antar, D. Roscoe, and M. Cuhaci, "Recent advances in dielectric resonator antenna technology," *IEEE Antennas Propag. Mag.*, Vol. 40, No. 3, 35–48, June 1998.
4. Luk, K. M. and K. W. Leung, *Dielectric Resonator Antennas*, Research Studies Press Ltd., Hertfordshire, U.K., 2002.
5. Mongia, R. K. and P. Bhartia, "Dielectric resonator antennas — A review and general design relations for resonant frequency and bandwidth," *Int. J. Microw. Millimeter-Wave Computer-Aided Eng.*, Vol. 4, No. 3, 230–247, 1994.
6. Petosa, A., *Dielectric Resonator Antennas Handbook*, Artech House, Boston, London, 2007.
7. Ge, Y. and K. P. Esselle, "A dielectric resonator antenna for UWB applications," *IEEE International Symposium on Antennas and Propagation Society*, 1–4, June 1–5, 2009.
8. Chair, R., A. A. Kishk, and K. F. Lee, "Wideband stair-shaped dielectric resonator antennas," *IET Microw, Antennas Propag.*, Vol. 1, No. 2, 299–305, 2007.
9. Kishk, A. A., B. Ahn, and D. Kajfez, "Broadband stacked dielectric resonator antennas," *Electronics Letters*, Vol. 25, No. 18, 1232–1233, 1989.
10. Kishk, A. A., X. Zhang, A. W. Glisson, and D. Kajfez, "Numerical analysis of stacked dielectric resonator antenna excited by a coaxial probe for wideband applications," *IEEE Transactions on Antennas and Propagation*, Vol. 51, No. 8, 1996–2005, August 2003.
11. Sharkawy, M. H. A., A. Z. Elsherbeni, and C. E. Smith, "Stacked elliptical dielectric resonator antennas for wideband," *Proc. IEEE*

- Antennas and Propagation Society Int. Symp.*, Vol. 2, 1371–1374, 2004.
12. Mongia, R. K., A. Ittipiboon, P. Bhartia, and M. Cuhaci, “Electric monopole antenna using a dielectric ring resonator,” *Elect. Lett.*, Vol. 29, No. 17, 1530–1531, August 19, 1993.
 13. Guha, D. and Y. M. M. Antar, “Four-element cylindrical dielectric resonator antenna for wideband monopole-like radiation,” *IEEE Transactions on Antennas and Propagation*, Vol. 54, No. 9, 2657–2662, September 2006.
 14. Chaudhary, R. K., K. V. Srivastava, and A. Biswas, “An investigation on three element multilayer cylindrical dielectric resonator antenna excited by a coaxial probe for wideband applications,” *Proceedings of IEEE Asia-Pacific Conference on Applied Electromagnetics (APACE)*, 2010.
 15. Guha, D. and Y. M. M. Antar, “New half-hemispherical dielectric resonator antenna for broadband monopole-type radiation,” *IEEE Transactions on Antennas and Propagation*, Vol. 54, No. 12, 3621–3628, December 2006.
 16. Guha, D., B. Gupta, and Y. M. M. Antar, “Quarter of a hemispherical dielectric resonator: New geometry explored to design a wideband monopole-type antenna,” *The XXIXth URSI General Assembly*, 2008.
 17. Gangwar, R. K., S. P. Singh, and D. Kumar, “Simulation study of four element rectangular dielectric resonator antenna array terminated in a bio-medium,” *IEEE Applied Electromagnetic Conference (AEMC)*, Kolkata, December 14–16, 2009.
 18. Lo, H. Y., K. W. Leung, K. M. Luk, and E. K. N. Yung, “Low profile equilateral-triangular dielectric resonator antenna of very high permittivity,” *Electronics Letters*, Vol. 35, No. 25, 2164–2166, December 9, 1999.
 19. Lo, H. Y. and K. W. Leung, “Excitation of low profile equilateral-triangular dielectric resonator antenna using a conductive conformal strip,” *Microwave and Optical Technology Letters*, Vol. 29, No. 5, 317–319, June 2001.
 20. Yoshihiko, A., “Operation modes of a waveguide Y circulator,” *IEEE Transactions on Microwave Theory and Techniques*, Vol. 23, 954–960, November 1974.
 21. Lo, H. Y., K. W. Leung, K. M. Luk, and E. K. N. Yung, “Low profile triangular dielectric resonator antenna,” Department of Electronic Engineering, City University of Hong Kong, 83 Tat Chee Avenue, Kowloon, Hong Kong SAR, China, 2000.